SIAM J. APPL. MATH.
Vol. 63, No. 4, pp. 1259–1275

EVANS FUNCTION STABILITY OF COMBUSTION WAVES*

V. GUBERNOV†, G. N. MERCER†, H. S. SIDHU†, AND R. O. WEBER†

Abstract. In this paper we investigate the linear stability and properties, such as speed, of the planar travelling combustion front. The speed of the front is estimated both analytically, using the matched asymptotic expansion, and numerically, by means of the shooting and relaxation methods. The Evans function approach extended by the compound matrix method is employed to numerically solve the linear stability problem for the travelling wave solution.

Key words. combustion waves, Evans function, compound matrix, Nyquist plot

AMS subject classifications. 35K57, 80A25

PII. S0036139901400240

1. Introduction.

Problems involving combustion waves are characterized by strong dependence of the reaction rate, which is usually modelled by the Arrhenius law, on the temperature. This sharp dependence of the reaction rate naturally divides the structure of the travelling front into three regions. Ahead of the combustion wave, in a preheat zone, the temperature is low and there is almost no reaction. When the temperature becomes sufficiently high, the reaction rate increases exponentially and the fuel is converted into heat very quickly. This takes place in a narrow region called the reaction zone. Finally, behind the front, in a product zone, all fuel is consumed, no reaction occurs, and the temperature is constant. The temperature and the amount of fuel change rapidly in the reaction zone. The above picture in some sense is close to the boundary layer problem. Therefore similar methods of analysis, like the matched asymptotic expansion (MAE), apply in both cases.

The analysis of steady propagating planar combustion fronts is usually based on MAE. According to this method, in the limit of high activation energy, we seek the travelling wave solution in the form of a series in all three regions; then on the boundaries of these zones the expansions are matched in each order of a small parameter. The asymptotic procedure in principle allows us to find the solution with any desired accuracy and for arbitrary Lewis number. As a rule, only the leading order is considered [1, 2, 3, 4, 5]; however, the higher order approximations can also be obtained [6]. The method of MAE is valid in the limit of large activation energy, and the properties of the steady combustion front, such as speed, can be found only numerically for general values of activation energy. Numerical analysis is mostly focused on solving the system of partial differential equations (PDE) that describe the problem [7, 8]. However, PDE can always be reduced to a system of ordinary differential equations (ODE) for steady propagating planar waves. In this paper we take advantage of the ODE formulation of the problem, which is usually more convenient for numerical analysis. We use shooting and relaxation methods to investigate the dependence of the speed of the front on the parameters of the problem. Besides the benefits of technical implementation, an ODE formulation does not depend on the

*Received by the editors December 28, 2001; accepted for publication (in revised form) October 2, 2002; published electronically April 9, 2003.
http://www.siam.org/journals/siap/63-4/40024.html
†School of Mathematics and Statistics, University of New South Wales at the Australian Defence Force Academy, Canberra, ACT 2600, Australia (vlad@ma.adfa.edu.au, g.mercer@adfa.edu.au, hss@ma.adfa.edu.au, r.weber@adfa.edu.au).

stability of the travelling wave and therefore allows us to continue the solution branch over a broader parameter range.

As we vary the parameters of the problem, a steady propagating planar front can lose stability, giving rise to either pulsating or cellular flames [5, 9]. Analytical investigation of the stability using the MAE leads to the so-called closure problem. In contrast to steady travelling waves, in this case the leading order equations depend on first order corrections, first order equations include second order terms of the asymptotic expansion, etc. In order to find the solution to the leading order problem, an infinite number of equations have to be investigated. One of the ways of overcoming this obstacle is just to truncate the expansion [1, 2, 3, 4, 5, 9]. This yields a closed problem with a replacement of the Arrhenius reaction rate by a delta-function source depending on the temperature at the reaction front. The truncated model has been used extensively for the stability analysis of combustion waves [1, 2, 3, 4]. However, the model with the delta-function source suffers from inconsistencies, as was noted in [5, 9]. The inverse of the small parameter of the expansion appears explicitly in the exponential terms describing the strength of the source. In other words, temperature variations behind the front are considered to be small in the exponential terms and of leading order elsewhere.

An asymptotically consistent approach was proposed in [5] for the system with the Lewis number of the order of unity. In this case the enthalpy does not change at the leading order. A closed problem was derived for the leading order temperature and the first order enthalpy. However, until recently [9], there has not been a consistent approach that treats the model with arbitrary Lewis number.

In [9] a generalization of the MAE method was introduced. The coefficients in the expansions are allowed to depend on the expansion parameter. This enables the correct scaling of the temperature variations ahead of and behind the reaction zone; namely, a restriction is imposed connecting the leading order temperature in the preheat zone and the first two terms of the asymptotic expansion in the product zone. The constraint reflects the fact that small temperature variations behind the front change the leading order terms in the preheat zone. The resulting model includes equations for the leading order variables ahead of the reaction zone and for the first order temperature variations in the product zone, together with matching and boundary conditions. There is no restriction on the range of the Lewis number values.

However, the models describing the propagation of the steady planar combustion waves were derived only in the leading order of the expansion parameter of the asymptotic procedure. In other words the papers mentioned above analyze the linear stability of models which are different from the original one with the Arrhenius kinetics. This is fully justified by the complexity of the problem and reveals the lack of alternative methods to MAE. Fortunately, recent advances in the application of the Evans function [10] to stability analysis of solitary waves and fronts [11, 12, 13, 14, 15] provide us with a powerful tool for the semianalytical investigation of travelling front stability.

The linear stability problem can always be formulated as an eigenvalue problem for some differential operator. The Evans function was first introduced in [10] to study the stability of nerve pulses as an analytical function whose zeros correspond to the isolated eigenvalues of this differential operator. In some specific cases the Evans function can be found explicitly, and the Evans function being zero gives the dispersion relation. In other cases, like solitary waves of a generalized Kordeweg–deVries (KdV) equation [16] and generalized nonlinear Schrödinger equation [17], the

asymptotic behavior of the Evans function can be found using the results obtained in [16], where the derivative of the Evans function was connected to the Melnikov integral [18]. The knowledge of asymptotics allowed the authors to localize zeros of the Evans function and to solve the stability problem analytically.

The asymptotic form of the Evans function for the combustion problem was derived in [15] in the limit of large activation energy and Lewis number of the order of unity. The results of [15] agree with the predictions of the MAE analysis of [5]. Zeros of the Evans function and therefore the stability of the combustion front can be found only numerically for general parameter values. Previously, this problem was solved by direct integration of the governing PDE [7, 8]. We cannot expect this method to be accurate near the critical parameter values, where the rate of instability is weak and a long integration time is needed to detect it. Furthermore, this method is relatively difficult for computational implementation in comparison with the numerical estimation of the Evans function proposed in [19], which is based on ODE integration. However, the latter method is applicable only for problems with a specific type of geometry, such as the linear stability problem for the KdV equation, and fails to work for stiff systems [12], such as in our case.

In the present paper we apply the Evans function method to the stability analysis of the planar combustion front. The linear stability problem associated with the travelling combustion wave is an example of a stiff problem. We extend the conventional algorithm for calculating the Evans function [19] by the compound matrix method [12, 13, 20, 21, 22], which was first employed for analysis of the hydrodynamic stability for the Orr–Sommerfeld equation. This method eliminates the stiffness and makes the linear stability problem numerically tractable.

In this paper we use the combination of shooting-relaxation and the Evans function method (extended by the compound matrix method) as a consistent approach for numerical investigation of both properties and stability of the travelling planar front, based on the ODE formulation of the combustion problem. We show that the method is valid for a wide range of the parameter values.

The paper is organized as follows. The model and governing equations are introduced in section 2. In section 3 we show how MAE can be used to derive travelling wave solutions in the limit of large activation energy, and we compare these solutions with the solutions obtained by shooting and relaxation methods. The linear stability problem is formulated in section 4, whereas the relation to the Evans function is discussed in section 5. In section 6 we quote the asymptotic results of [15] for the Evans function. Numerical stability analysis is carried out in section 7. Finally, concluding remarks can be found in section 8.

2. Model. We consider a premixed fuel in one dimension. The heat loss is neglected. We assume that the rate of exothermic combustion is well described by the Arrhenius law. In nondimensional coordinates, the equations governing this process can be found in [7] and are given as

$$u_t = u_{xx} + ve^{-1/u}, \qquad v_t = \tau v_{xx} - \beta ve^{-1/u}, \tag{2.1}$$

where u and v are the nondimensional temperature and mass fraction of the fuel, respectively; τ is the inverse Lewis number (the ratio of the diffusion rates of mass and heat); and β is the ratio of the activation energy to heat release.

We consider the ambient temperature to be equal to zero. This approximation simplifies the problem, decreasing the number of parameters. As is noted in [7], this is a way to circumvent the "cold-boundary problem" and does not change the behavior of

the system. It is not an appropriate simplification when considering ignition problems. Parameter τ varies from zero, for solid fuel, to unity, for gaseous fuels. The parameter β is of the order of unity or larger.

We consider system (2.1) subject to the following boundary conditions:

$$\begin{array}{llll} u(x,t) \to \beta^{-1}, & v(x,t) \to 0 & \text{as} & x \to -\infty, \\ u(x,t) \to 0, & v(x,t) \to 1 & \text{as} & x \to +\infty. \end{array} \tag{2.2}$$

On the right boundary we have a cold ($u = 0$) and unburned ($v = 1$) state, whereas the opposite limit corresponds to the hot ($u = \beta^{-1}$) and burned ($v = 0$) state.

3. Travelling wave solution. Let us consider the case $\tau \sim O(1)$. We will seek the solution of (2.1) in a form of the front travelling with a constant speed c

$$u(x,t) = u(\xi), \qquad v(x,t) = v(\xi), \tag{3.1}$$

where we have introduced a moving coordinate frame $\xi = x - ct$. After substituting (3.1) into (2.1), it is easy to obtain two second order differential equations

$$u_{\xi\xi} + cu_\xi + ve^{-1/u} = 0, \qquad \tau v_{\xi\xi} + cv_\xi - \beta ve^{-1/u} = 0 \tag{3.2}$$

and boundary conditions

$$\begin{array}{llll} u = \beta^{-1}, & v = 0 & \text{as} & \xi \to -\infty, \\ u = 0, & v = 1 & \text{as} & \xi \to +\infty. \end{array} \tag{3.3}$$

Now let us make the reaction terms in (3.1) symmetric by introducing new variables $\widetilde{u} = \beta u$, $\widetilde{v} = v$ and scale the coordinate $z = c\xi$. This gives us the equations

$$\widetilde{u}_{zz} + \widetilde{u}_z + \beta^2 Q\widetilde{v}e^{\beta(1-1/\widetilde{u})} = 0, \qquad \tau\widetilde{v}_{zz} + \widetilde{v}_z - \beta^2 Q\widetilde{v}e^{\beta(1-1/\widetilde{u})} = 0, \tag{3.4}$$

where $Q = (\beta c^2 e^\beta)^{-1}$ is a flame speed eigenvalue, which has to be found. Boundary conditions are modified as follows:

$$\begin{array}{llll} \widetilde{u} = 1, & \widetilde{v} = 0 & \text{as} & z \to -\infty, \\ \widetilde{u} = 0, & \widetilde{v} = 1 & \text{as} & z \to +\infty. \end{array} \tag{3.5}$$

In the new variables the reaction zone is of the order of β^{-1}. Outside this zone the reaction terms of (3.4) become negligible. Hence in the outer region (3.4) can be written as

$$\widetilde{u}_{zz} + \widetilde{u}_z = 0, \qquad \tau\widetilde{v}_{zz} + \widetilde{v}_z = 0, \tag{3.6}$$

subject to boundary conditions (3.5).

We seek the solution of problem (3.6) in the form of a series, with β^{-1} being a small parameter, and hence we postulate

$$\begin{aligned} \widetilde{u} &= U_0 + \beta^{-1}U_1 + \cdots, \\ \widetilde{v} &= V_0 + \beta^{-1}V_1 + \cdots, \\ Q &= Q_0 + \beta^{-1}Q_1 + \cdots. \end{aligned} \tag{3.7}$$

In the zeroth order, the solution of equations (3.6) is

$$U_0 = \begin{cases} 1, & z < 0, \\ e^{-z}, & z > 0, \end{cases} \quad \text{and} \quad V_0 = \begin{cases} 0, & z < 0, \\ 1 - e^{-z/\tau}, & z > 0. \end{cases} \tag{3.8}$$

In order to find Q_0 we should match the solution (3.8) with the solution of the inner problem.

Let us consider (3.4) in a thin boundary layer where the reaction occurs. We introduce the stretched coordinate $y = \beta z$ and seek solutions of the form

$$\begin{aligned} \widetilde{u} &= 1 + \beta^{-1}u_1 + \beta^{-2}u_2 + \cdots, \\ \widetilde{v} &= \beta^{-1}v_1 + \beta^{-2}v_2 + \cdots, \\ Q &= Q_0 + \beta^{-1}Q_1 + \cdots. \end{aligned} \tag{3.9}$$

After substituting (3.9) into (3.4) and leaving the leading terms of the order $O(\beta)$, we obtain the equations

$$\ddot{u}_1 + Q_0 v_1 e^{u_1} = 0, \qquad \tau\ddot{v}_1 - Q_0 v_1 e^{u_1} = 0, \tag{3.10}$$

with the dot denoting derivative $\partial/\partial y$. In deriving (3.10) we have assumed that $\tau \sim O(1)$ and $Q_0 \sim O(1)$. On the boundaries we can require that the following matching conditions be satisfied:

$$\begin{aligned} &\lim_{y\to\pm\infty}[u_1(y) - U_1(0\pm) - U_{0z}(0\pm)y] = 0, \\ &\lim_{y\to\pm\infty}[v_1(y) - V_1(0\pm) - V_{0z}(0\pm)y] = 0. \end{aligned} \tag{3.11}$$

On the left boundary from (3.8) it follows that $U_{0z}(0-) = V_{0z}(0-) = 0$, and we can rewrite (3.11) in the form

$$\begin{aligned} &u_1 = U_1(0-), \quad v_1 = V_1(0-) \\ &\dot{u}_1 = 0, \qquad\quad \dot{v}_1 = 0 \end{aligned} \qquad \text{as} \quad y \to -\infty. \tag{3.12}$$

System (3.10) has the integral

$$u_1 + \tau v_1 = C_1 + D_1 y. \tag{3.13}$$

Applying the matching condition (3.12), it can be shown that $D_1 = 0$ and $C_1 = U_1(0-) + \tau V_1(0-)$. Using this integral system, (3.10) can be reduced to a single equation

$$\ddot{\theta} - k\theta e^{-\theta} = 0, \tag{3.14}$$

where $\theta = C_1 - u_1$, $k = Q_0/\tau e^{C_1}$. Equation (3.14) can be treated as the equation of motion of a point particle with unit mass in the potential $W(\theta) = k(1+\theta)e^{-\theta}$. The potential $W(\theta)$ has a maximum only for $\theta = 0$. Conditions (3.12) imply that $\dot{\theta}(-\infty) = 0$. This is possible only if the energy $E = \dot{\theta}^2/2 + W(\theta)$ is equal to the maximal value of the potential $W(0) = k$. Therefore, $\theta = 0$ as $y \to -\infty$, and consequently, $C_1 = U_1(0-)$ and $V_1(0-) = 0$. On the other hand, as $y \to +\infty$ the potential $W(y)$ decays exponentially and $\dot{\theta} \to \sqrt{2k}$.

Returning to the original problem, the left boundary conditions can be written as

$$\begin{aligned} &u_1 = U_1(0-), \quad v_1 = 0 \\ &\dot{u}_1 = 0, \qquad\quad \dot{v}_1 = 0 \end{aligned} \qquad \text{as} \quad y \to -\infty. \tag{3.15}$$

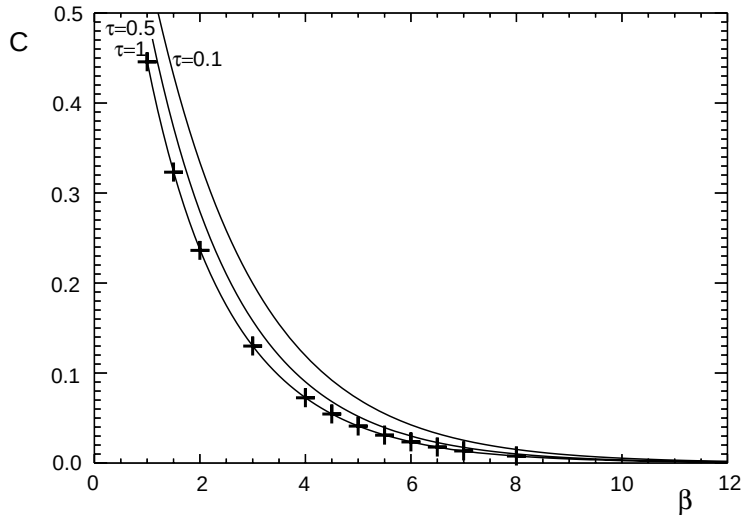

FIG. 1. *Numerically determined speed of the travelling front as a function of β. Solid lines correspond to the results obtained by shooting and relaxation methods for values of parameter $\tau =$ 0.1, 0.5, and 1.0 (right to left). Crosses represent the speed of the front calculated by direct PDE integration of* (2.1) *for* $\tau = 1.0$.

On the right boundary, it follows from (3.11) and (3.13) that

$$\left(\frac{\partial U_0}{\partial z}\right)_{z=0+} = -\tau \left(\frac{\partial V_0}{\partial z}\right)_{z=0+} = -\sqrt{\frac{2Q_0}{\tau e^{U_1(0-)}}}. \tag{3.16}$$

For planar front solution $U_1(0-) = 0$ and from (3.8) we have $(\partial U_0/\partial z)_{z=0+} = -1$. Taking into account the definition of Q, we can obtain the following estimation of the speed:

$$c = \sqrt{2\tau^{-1}\beta^{-1}} e^{-\beta/2}, \tag{3.17}$$

which agrees with the results of [7, 8] in the limit of large β. Note that a similar expression for the front speed was first found in [6].

We also solved (3.2) numerically. As in [23], we used the shooting method to obtain the guess solution, and then the results were corrected with a more accurate method, namely, relaxation. Combination of these methods allowed us to numerically obtain the dependence of the travelling front velocity on the parameters β and τ. In Figure 1 we plot the speed of the front as a function of β for three different values of τ. The results are compared to the predictions obtained in [7] by direct PDE integration of (2.1). The accordance between these two approaches is excellent.

In Figure 2 we compare the prediction of the asymptotic formula (3.17) for the speed of the front with the results obtained numerically. As can be seen, the correspondence is quite good for $\tau = 1$ and large values of β. However, when we decrease the value of τ, the approximation of the speed (3.17), which is valid for $\tau \sim O(1)$, becomes unsatisfactory. For example, when $\tau = 0.1$, the difference between the analytical and numerical results becomes significant.

The stability analysis of the steady propagating combustion front carried out in the following sections is based on how accurately we can approximate the solution of

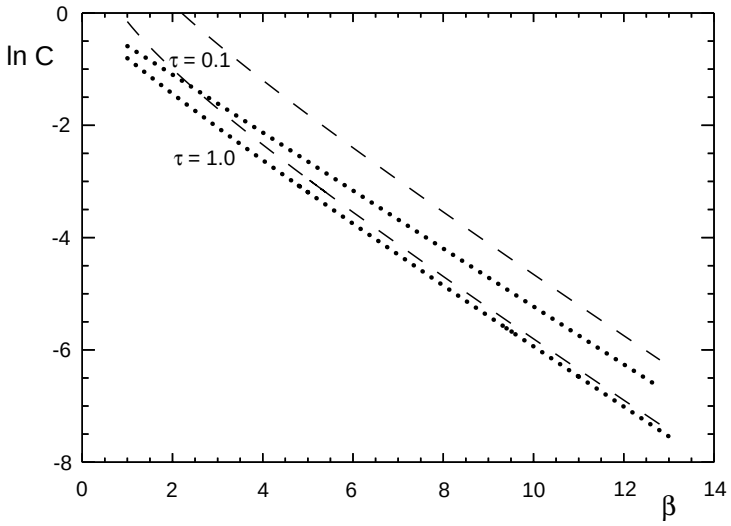

FIG. 2. *Logarithm of the speed of the travelling front as a function of β for values of parameter $\tau = 0.1$ and 1.0. Dots correspond to the numerical results, whereas dashed lines represent the approximation of the speed according to the formula* (3.17). *In each case the upper line is for $\tau = 0.1$ and the lower line for $\tau = 1.0$.*

(3.2). Standard relaxation routine (see [23] and references therein) allows us to control the average local correction made on each iteration step. The solution is considered to be resolved if the correction is less than 10^{-15}. We also tested the accuracy of the method independently by changing the step of the grid and comparing the resulting variations in the values of the front speed. For example, a fourfold mesh refinement changes the value of the front speed in the ninth significant digit. Therefore we assume that the numerical procedure outlined here works reasonably well.

4. Stability of a travelling front. As a first step in the analysis of travelling wave stability, we linearize (2.1) around the front solution (3.1):

$$u(x,t) = u(\xi) + \varphi(\xi,t), \qquad v(x,t) = v(\xi) + \chi(\xi,t), \tag{4.1}$$

where φ and χ are linear perturbation terms. After substitution of (4.1) into (2.1) it is straightforward to derive

$$\begin{pmatrix} \partial\varphi/\partial t \\ \partial\chi/\partial t \end{pmatrix} = \hat{L} \begin{pmatrix} \varphi \\ \chi \end{pmatrix}, \tag{4.2}$$

where

$$\hat{L} = \begin{pmatrix} \partial_\xi^2 + vu^{-2}e^{-1/u} + c\partial_\xi & e^{-1/u} \\ -\beta vu^{-2}e^{-1/u} & \tau\partial_\xi^2 - \beta e^{-1/u} + c\partial_\xi \end{pmatrix}. \tag{4.3}$$

The stability of the travelling front is then defined from the spectra of $\hat{L}$. It is easy to show that the essential spectrum of this operator always lies in the left half-plane and therefore the discrete spectrum is solely responsible for the transition to instability (see [24]). We will seek the solution of (4.2) of the form

$$\varphi(\xi,t) = \varphi(\xi)e^{\lambda t}, \qquad \chi(\xi,t) = \chi(\xi)e^{\lambda t}, \tag{4.4}$$

where λ is a spectral parameter (in combustion literature it is sometimes referred to as the growth rate eigenvalue). Substituting (4.4) into (4.2) and introducing a vector with the components $z_1 = \varphi,\ z_2 = \varphi_\xi,\ z_3 = \chi,\ z_4 = \chi_\xi$, we obtain the system of ODE in the form

$$\dot{\mathbf{z}} = \mathbf{A}\mathbf{z}, \tag{4.5}$$

where

$$\mathbf{A}(\xi,\lambda) = \begin{pmatrix} 0 & 1 & 0 & 0 \\ \lambda - vu^{-2}e^{-1/u} & -c & -e^{-1/u} & 0 \\ 0 & 0 & 0 & 1 \\ \beta\tau^{-1}vu^{-2}e^{-1/u} & 0 & \tau^{-1}(\lambda + \beta e^{-1/u}) & -\tau^{-1}c \end{pmatrix}. \tag{4.6}$$

We use (4.5) to investigate the stability of the travelling front. Following [12], we will say that the travelling front is linearly unstable if, for some fixed complex λ with $Re(\lambda) > 0$, there exists a solution of (4.5) which decays exponentially as $\xi \to \pm\infty$. We will refer to this λ as an eigenvalue and to the corresponding solution as an eigenmode.

5. Evans function. Let us introduce the limit matrices

$$\mathbf{A}_\pm(\lambda) \equiv \lim_{\xi\to\pm\infty} \mathbf{A}(\xi,\lambda). \tag{5.1}$$

The explicit form of $\mathbf{A}_\pm$ can be found from the boundary conditions (3.3). The limit matrices have eigenvalues

$$\begin{aligned} &\mu^-_{1,2}(\lambda) = \tfrac{-c\mp\sqrt{c^2+4\lambda}}{2}, && \mu^+_{1,2} = \mu^-_{1,2}, \\ &\mu^-_{3,4}(\lambda) = \tfrac{-c\mp\sqrt{c^2+4\tau(\lambda+\beta e^{-\beta})}}{2\tau}, && \mu^+_{3,4}(\lambda) = \mu^-_{3,4}(\lambda - \beta e^{-\beta}), \end{aligned} \tag{5.2}$$

with corresponding eigenvectors $\mathbf{k}^\pm_i$ (for $i = 1,\dots,4$). Equations (5.2) imply that $\mathbf{A}_-$ has two eigenvalues $\mu^-_{2,4}$ with positive real parts and two eigenvalues $\mu^-_{1,3}$ with negative real parts. Similarly, for $\mathbf{A}_+$ we have $Re(\mu^+_{2,4}) > 0$ and $Re(\mu^+_{1,3}) < 0$. Therefore, for any value of λ there exist two linearly independent solutions $\mathbf{z}^-_{2,4}(\xi,\lambda)$ of (4.5) corresponding to unstable subspaces of $\mathbf{A}_-$ satisfying the conditions

$$\lim_{\xi\to-\infty} \exp(-\mu^-_i\xi)\mathbf{z}^-_i(\xi,\lambda) = \mathbf{k}^-_i, \qquad i = 2,4, \tag{5.3}$$

and two linearly independent solutions $\mathbf{z}^+_{1,3}(\xi,\lambda)$ of (4.5) corresponding to stable subspaces of $\mathbf{A}_+$ satisfying the conditions

$$\lim_{\xi\to+\infty} \exp(-\mu^+_i\xi)\mathbf{z}^+_i(\xi,\lambda) = \mathbf{k}^+_i, \qquad i = 1,3. \tag{5.4}$$

Now we can consider a space of solutions of (4.5) bounded as $\xi \to -\infty$ and a space of solutions bounded as $\xi \to +\infty$. If these spaces intersect nontrivially for some value λ, then λ is an eigenvalue. We will call the function which measures whether these spaces intersect the Evans function. Geometrically this means that for some value of λ and any value of coordinate ξ the plane defined by the vectors $\mathbf{z}^-_{2,4}$ intersects nontrivially with the plane defined by the vectors $\mathbf{z}^+_{1,3}$. We can also say that λ is an eigenvalue if and only if the solutions $\mathbf{z}^-_{2,4}$ and $\mathbf{z}^+_{1,3}$ are linearly dependent or, equivalently, the Wronskian evaluated on these solutions (a matrix whose columns

are $\mathbf{z}^-_{2,4}(\xi)$ and $\mathbf{z}^+_{1,3}(\xi)$) is equal to zero. One of the Evans function definitions is given in [15] via this Wronskian, which is evaluated for definiteness at $\xi = 0$. Let $\mathbf{e}_i$ be the orthonormal basis in four dimensional space $\mathbf{C^4}$ of system (4.5) solutions. In this basis the vectors $\mathbf{z}^\pm_i$ have coordinates $(z^\pm_{i1}, z^\pm_{i2}, z^\pm_{i3}, z^\pm_{i4})^T$, and the Evans function is defined as

$$D(\lambda) = \begin{vmatrix} z^-_{21}(0,\lambda) & z^-_{41}(0,\lambda) & z^+_{11}(0,\lambda) & z^+_{31}(0,\lambda) \\ z^-_{22}(0,\lambda) & z^-_{42}(0,\lambda) & z^+_{12}(0,\lambda) & z^+_{32}(0,\lambda) \\ z^-_{23}(0,\lambda) & z^-_{43}(0,\lambda) & z^+_{13}(0,\lambda) & z^+_{33}(0,\lambda) \\ z^-_{24}(0,\lambda) & z^-_{44}(0,\lambda) & z^+_{14}(0,\lambda) & z^+_{34}(0,\lambda) \end{vmatrix}. \tag{5.5}$$

In what follows we will also require an alternative definition of the Evans function. Returning to the geometrical picture, we can say that to find the eigenvalues we do not have to seek the solutions $\mathbf{z}^-_{2,4}$ and $\mathbf{z}^+_{1,3}$, but it is sufficient to determine the orientation of the planes, constructed on corresponding pairs of vectors, in space $\mathbf{C^4}$ of system (4.5) solutions.

If we take two linear independent vectors in $\mathbf{C^n}$, then the orientation of a plane containing both vectors can be determined by a wedge product of them. (Two vectors are linear dependent if and only if their wedge product is equal to zero.) If $n = 3$, a wedge product coincides with a vector product, and the result of the operation is a vector belonging to $\mathbf{C^3}$. However, in the general case the result of a wedge product of two vectors is a vector lying in $\bigwedge^2(\mathbf{C^n})$, where $\bigwedge^2(\mathbf{C^n})$ is the second exterior power of $\mathbf{C^n}$. It has dimension $\dim[\bigwedge^2(\mathbf{C^n})] = n!/2!(n-2)!$.

In our case a plane can be defined by a six component vector; for instance, we define

$$\mathbf{V}^- = \mathbf{z}^-_2 \wedge \mathbf{z}^-_4, \qquad \mathbf{V}^+ = \mathbf{z}^+_1 \wedge \mathbf{z}^+_3, \tag{5.6}$$

where $\mathbf{V}^\pm \in \bigwedge^2(\mathbf{C^4})$ and $\wedge$ stands for wedge product. If λ is an eigenvalue, the planes associated with the vectors $\mathbf{V}^+$ and $\mathbf{V}^-$ intersect nontrivially. This means that $\mathbf{V}^+$ and $\mathbf{V}^-$ are linear dependent and a wedge product $\mathbf{V}^+ \wedge \mathbf{V}^-$ equals zero. Now we can make use of the Evans function definition given in [25] as

$$\widetilde{D}(\lambda) = \exp\left[-\int_0^\xi Tr(\mathbf{A}(s,\lambda))\right] \mathbf{V}^+(\xi,\lambda) \wedge \mathbf{V}^-(\xi,\lambda). \tag{5.7}$$

For the sake of further consideration it is convenient to take $\xi = 0$ in the definition (5.7). As was shown in [12], in this case we can rewrite (5.7) as

$$\widetilde{D}(\lambda) = D(\lambda)\Gamma, \tag{5.8}$$

where $\Gamma = \mathbf{e}_1 \wedge \mathbf{e}_2 \wedge \mathbf{e}_3 \wedge \mathbf{e}_4$ is a standard volume in $\mathbf{C^4}$ and

$$D(\lambda) = [\mathbf{V}^+, \Sigma\overline{\mathbf{V}^-}]. \tag{5.9}$$

Here, the overline denotes the complex conjugate, $[\cdot,\cdot]$ is the complex inner product in $\mathbf{C^6}$, and Σ is the operator that in a basis

$$\begin{aligned} &\mathbf{v}_1 = \mathbf{e}_1 \wedge \mathbf{e}_2, \quad \mathbf{v}_2 = \mathbf{e}_1 \wedge \mathbf{e}_3, \quad \mathbf{v}_3 = \mathbf{e}_1 \wedge \mathbf{e}_4, \\ &\mathbf{v}_4 = \mathbf{e}_2 \wedge \mathbf{e}_3, \quad \mathbf{v}_5 = \mathbf{e}_2 \wedge \mathbf{e}_4, \quad \mathbf{v}_6 = \mathbf{e}_3 \wedge \mathbf{e}_4, \end{aligned} \tag{5.10}$$

is represented by the matrix

$$\Sigma = \begin{pmatrix} 0 & 0 & 0 & 0 & 0 & 1 \\ 0 & 0 & 0 & 0 & -1 & 0 \\ 0 & 0 & 0 & 1 & 0 & 0 \\ 0 & 0 & 1 & 0 & 0 & 0 \\ 0 & -1 & 0 & 0 & 0 & 0 \\ 1 & 0 & 0 & 0 & 0 & 0 \end{pmatrix}. \tag{5.11}$$

In the basis (5.10) the components of vector $\mathbf{V}^-$ can be shown to be

$$\begin{array}{ll} \mathbf{V}_1^- = z_{21}z_{42} - z_{41}z_{22}, & \mathbf{V}_4^- = z_{22}z_{43} - z_{42}z_{23}, \\ \mathbf{V}_2^- = z_{21}z_{43} - z_{41}z_{23}, & \mathbf{V}_5^- = z_{22}z_{44} - z_{42}z_{24}, \\ \mathbf{V}_3^- = z_{21}z_{44} - z_{41}z_{24}, & \mathbf{V}_6^- = z_{23}z_{44} - z_{43}z_{24}. \end{array} \tag{5.12}$$

A similar relation holds for $\mathbf{V}^+$. Using these expressions for $\mathbf{V}^\pm$, we can show (by means of direct substitution) that definitions (5.5) and (5.9) are identical.

The vectors $\mathbf{V}^\pm$ can be also called the second compounds of the matrices formed from a pair $\mathbf{z}_{2,4}^-$ or $\mathbf{z}_{1,3}^+$, respectively, and were considered in [20, 21, 22] in relation with the Orr–Sommerfeld equation. The definition (5.5) is the simpler of the two, but the importance of the second definition (5.9) will be revealed in section 7.

6. Evans function for $\tau \sim O(1)$ and $\beta \gg 1$. Let us return to the definition (5.5) of the Evans function. In [15] it was shown that in the case of $\tau \sim 1$ and $\beta \gg 1$ the Evans function can be approximated analytically with good accuracy. In this section we assume that $\tau = 1 - \beta^{-1}\ell$, where $\ell \sim 1$.

First, let us rewrite the spectral problem (4.2)–(4.3) for the operator $\hat{L}$ in the symmetric form. By introducing the variables $\widetilde{u} = \beta u$, $\widetilde{v} = v$, $\widetilde{\varphi} = \beta\varphi$, $\widetilde{\chi} = \chi$, and the scaled coordinate $z = c\xi$ defined in section 3, we can obtain

$$\hat{L}\begin{pmatrix} \widetilde{\varphi} \\ \widetilde{\chi} \end{pmatrix} = \widetilde{\lambda}\begin{pmatrix} \widetilde{\varphi} \\ \widetilde{\chi} \end{pmatrix}, \tag{6.1}$$

where $\widetilde{\lambda} = \lambda/c^2$ and

$$\hat{L} = \begin{pmatrix} \partial_z^2 + \partial_z + \beta^3 Q\widetilde{v}\widetilde{u}^{-2}e^{\beta(1-1/\widetilde{u})} & \beta^2 Q e^{\beta(1-1/\widetilde{u})} \\ -\beta^3 Q\widetilde{v}\widetilde{u}^{-2}e^{\beta(1-1/\widetilde{u})} & \tau\partial_z^2 + \partial_z - \beta^2 Q e^{\beta(1-1/\widetilde{u})} \end{pmatrix}. \tag{6.2}$$

A similar type of equation was considered in [15]. The solutions $\widetilde{\mathbf{z}}_{2,4}^-$ and $\widetilde{\mathbf{z}}_{1,3}^+$ of (6.1), having the same meaning as in the previous section, were found. Using the definition (5.5), the Evans function can be shown to be approximated in the limit $\beta \to \infty$ as

$$D(\widetilde{\lambda}, \ell) = 2\Gamma^2(\Gamma - 1) - \ell(2\widetilde{\lambda} - \Gamma + 1), \tag{6.3}$$

where $\Gamma = \sqrt{1 + 4\widetilde{\lambda}}$. As ℓ crosses $\ell_c = 4(1+\sqrt{3}) \approx 10.92$, a pair of complex conjugate eigenvalues $\pm i\widetilde{\lambda}_c$, where $\widetilde{\lambda}_c \approx 0.6356$, passes into the right half of the complex plane, giving rise to a Hopf bifurcation. The same result was obtained in [4, 5] using the matched asymptotic expansion. Now we can estimate the boundary of stability of the planar front as $\beta = \ell_c/(1-\tau)$ and the Hopf frequency $\lambda = c^2\widetilde{\lambda}_c$. Unfortunately, we cannot expect this prediction to be quantitatively accurate, because in the beginning of the consideration it was assumed that $\ell \sim O(1)$, whereas ℓ_c has been found to be much greater.

7. Numerics and the compound matrix method. The method of calculating the Evans function was proposed in [19]. The idea is based on the definition (5.5). According to (5.5) it is necessary to determine the solutions $\mathbf{z}^-_{2,4}$ or $\mathbf{z}^+_{1,3}$ at $\xi = 0$. In order to numerically trace the solution, for example, growing as we integrate forward, the coordinate is exponentially scaled so as to eliminate the maximal rate of exponential growth. However, the numerical algorithm introduced in [19] allows us to find only the solutions which correspond to maximal (minimal) rates of exponential growth (decay) as $\xi \to \pm\infty$.

In our case we need to obtain two pairs of solutions: one pair bounded as ξ tends to $+\infty$, another as $\xi \to -\infty$. Let us consider for definiteness $\xi < 0$. From the analysis developed in section 5 it follows that system (4.5) has two solutions $\mathbf{z}^-_{2,4}$ bounded as $\xi \to -\infty$ and two solutions $\mathbf{z}^-_{1,3}$ unbounded as $\xi \to -\infty$ which are of no interest. In order to neglect $\mathbf{z}^-_{1,3}$ we have to numerically integrate the system (4.5) from $\xi = -l_1$ to $\xi = 0$ (where l_1 is chosen sufficiently large). Integrating forward we can find only $\mathbf{z}^-_4$, because $\mu^-_2 < \mu^-_4$ and the solution $\mathbf{z}^-_2$ is always ruled out due to errors of the numerical scheme. The same obstacles remain in the limit $\xi \to +\infty$. Systems with this kind of behavior are called stiff. The stiffness makes the direct calculation using (5.5) impossible, and some procedure of orthogonalization is required. The compound matrix method, which we employed in order to avoid this type of difficulty, is described below and will be seen to be closely related to the definition (5.9) introduced in section 5.

Let $\mathbf{z}_1$ and $\mathbf{z}_2$ be two solutions of (4.5); then the vector $\mathbf{V} = \mathbf{z_1} \wedge \mathbf{z_2}$ is the solution of the equation

$$\dot{\mathbf{V}} = \mathbf{B}\mathbf{V}, \tag{7.1}$$

where $\mathbf{B}$ is a 6×6 matrix whose elements can be found from the matrix $\mathbf{A}$ (see [13, 20, 21, 22] for details). It can be shown that the eigenvalues $s^\pm_i$ of $\mathbf{B}$ in the limits $\xi = \pm\infty$ are given via eigenvalues $\mu^\pm_i$ of $\mathbf{A}_\pm$ as

$$\begin{aligned} s^\pm_1 &= \mu^\pm_1 + \mu^\pm_2, \quad s^\pm_4 = \mu^\pm_2 + \mu^\pm_3, \\ s^\pm_2 &= \mu^\pm_1 + \mu^\pm_3, \quad s^\pm_5 = \mu^\pm_2 + \mu^\pm_4, \\ s^\pm_3 &= \mu^\pm_1 + \mu^\pm_4, \quad s^\pm_6 = \mu^\pm_3 + \mu^\pm_4. \end{aligned} \tag{7.2}$$

Therefore $\mathbf{V}^-(\xi)$, defined by (5.6), is the solution of (7.1) corresponding to the largest rate of exponential growth s^-_5 as we integrate forward from $\xi = -\infty$ to $\xi = 0$. Similarly $\mathbf{V}^+(\xi)$, defined by (5.6), is the solution of (7.1) corresponding to the largest rate of exponential growth s^+_2 as we integrate backward from $\xi = +\infty$ to $\xi = 0$. These solutions can always be found numerically by means of the method introduced in [19], and then we use definition (5.9) to calculate the Evans function numerically.

The problem of stability of the travelling front of (2.1) then reduces to the search for zeros of the Evans function (5.9) located in the right half-plane. Zeros of $D(\lambda)$ can be calculated using an argument principle. The number of zeros in the right half-plane equals the number of times the image of the imaginary axis under $D(it)$, $t \in R$, winds (wraps) around the origin. Graphs of $D(it), t \in R$, are called Nyquist plots [19].

Figure 3 shows Nyquist plots for $\tau = 0.1$ and $\beta = 6.8,\ 7.026,\ 7.2$. For $\beta = 6.8$ the curve does not encircle the origin, and hence the travelling front is stable. Transition to instability occurs for $\beta = 7.026$, when two complex conjugate eigenvalues cross the imaginary axes and the curve passes through the origin three times. The front

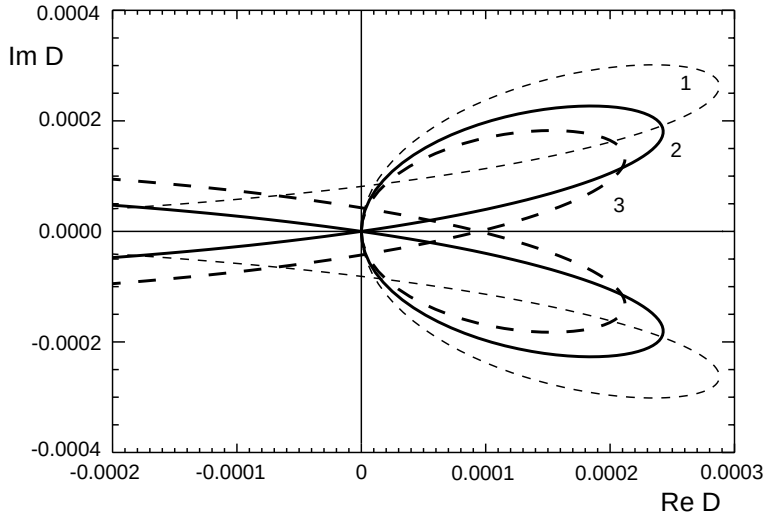

FIG. 3. *Transition to instability. The image of the imaginary axis $D(it)$ near the origin for $\tau = 0.1$ and for $\beta = 6.8$ (curve 1), 7.026 (curve 2), 7.2 (curve 3). Note that curve 1 does not encircle the origin, curve 2 is the transition, and curve 3 encircles the origin two times.*

is clearly unstable for $\beta = 7.2$, when the curve encircles the origin two times, and therefore there are two points of discrete spectra in the right half-plane.

The Nyquist plot technique allows us to obtain the criterion of transition to instability. Using this criterion, we can conclude whether the travelling front is stable or not for some fixed parameter values. However, it is quite difficult to calculate the critical parameter values. More detailed information can be collected by means of the Newton–Raphson method, which we apply to the equation $D(\lambda) = 0$. This allows us to locate the zeros of the Evans function on the complex plane for any given values of β and τ. In Figure 4 it is shown how two complex conjugate eigenvalues move from the left half-plane to the right half-plane, resulting in Hopf bifurcation at the parameter values when λ is purely imaginary. To determine the critical value β_c, when a pair of eigenvalues is located exactly on the imaginary axis, we consider the equation $Re\lambda = 0$ together with $D(\lambda) = 0$ and solve this system using the Newton–Raphson method. We start the iteration process with appropriate guess values for λ and β. We repeat the process until the zero is found with an accuracy of 10^{-12}. This gives us $\beta_c = 7.02609...$ for $\tau = 0.1$. While searching for the zeros of the Evans function, we checked the credibility of the method by decreasing the integration step by a factor of four. This results in the variation of the critical value of β in the ninth significant figure.

It is clear that we can use the procedure described above to find the dependence of the critical value β_c on τ. In Figure 5 the stability boundary is plotted in the parameter plane (β, τ). In section 6 we showed that as we increase τ towards 1, the corresponding value β_c tends to infinity. At the same time, according to (3.17) and the results of section 6, the speed of the front and the Hopf frequency tends to zero. As a result, the travelling front becomes flatter, and we should infinitely increase the interval of integration. For example, when $\tau = 0.6$, the critical values become $\beta_c = 21.087$, $c = 9.509 \times 10^{-6}$, $\lambda_c = 6.969 \times 10^{-11}$, and the interval of integration is about 10^6. In addition, it is numerically difficult to trace such small

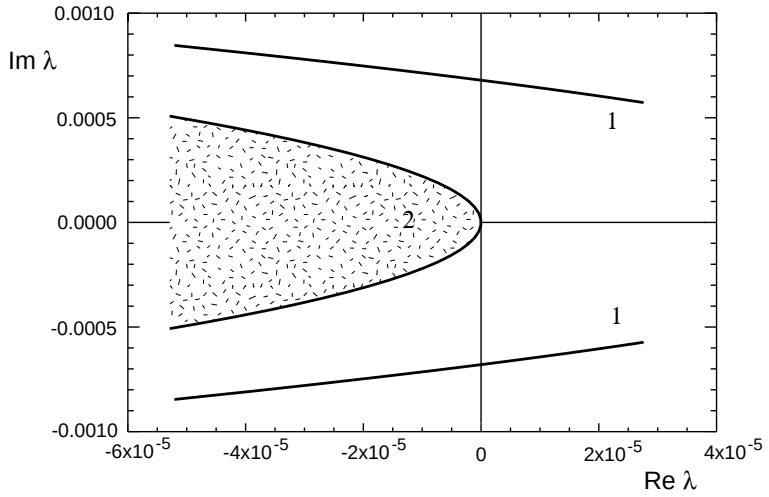

FIG. 4. *The spectra of operator* $\hat{L}$ *for* $\tau = 0.1$ *and* β *in the range* [6.8, 7.2]. *Curves* 1 *denote the location of eigenvalues for different values of* β. *Curve* 2 *is the boundary of the region where the essential spectrum lies. The value of* β *at which curves* 1 *pass through the imaginary axis gives the critical value* β_c.

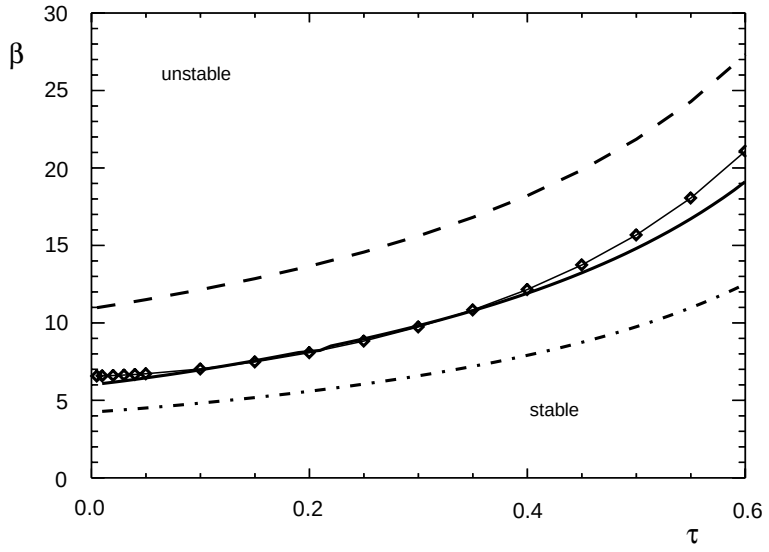

FIG. 5. *Stability boundary* $\beta_c(\tau)$. *Dots connected with a thin solid curve are the results of numerical calculations based on the Evans function. Other lines represent the analytical predictions obtained with* (1) *dash line—Evans function asymptotic from section* 6, (2) *dash-dot line—truncation model,* (3) *thick solid line—generalized MAE.*

values of λ_c. This implies that we can find the boundary of stability only on the interval $\tau \in [0, 0.6]$. As a result, it is extremely difficult to verify the asymptotic formula for $\beta_c(\tau)$ derived in section 6, as this is valid for $\tau \sim 1$. In Figure 5 we also plot the prediction obtained with the truncation model [9]. As can be seen, the discrepancy between the theoretical and numerical results is large for both asymptotic models. The generalized MAE developed in [9] gives the best correspondence with

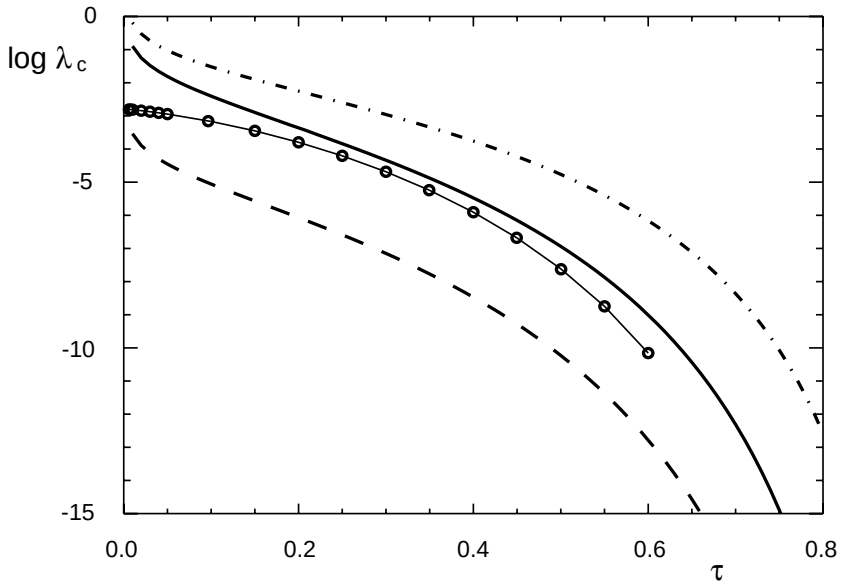

FIG. 6. *The logarithm of the Hopf frequency as a function of τ. Dots connected with a thin solid curve correspond to numerical results. Other lines represent the analytical predictions obtained with* (1) *dash line—Evans function asymptotic from section* 6, (2) *dash-dot line—truncation model,* (3) *thick solid line—generalized MAE.*

the numerical data for $\tau \in [0.1, 0.5]$. In Figure 6 we plot the logarithm of the Hopf frequency as a function of τ for $\beta = \beta_c$. As in the previous figure, the generalized MAE estimation best fits the numerical results.

Finally, using the compound matrix method, we can find the eigenmodes of the system (4.2)–(4.3) by inverting the relations (5.12) for $\mathbf{V}^-$ and similarly for $\mathbf{V}^+$. In Figures 7 and 8 we show the eigenmodes obtained for $\tau = 0.3$ for the critical value $\beta_c = 9.7404$, when two eigenvalues lie on the imaginary axis. These eigenmodes can be used, for example, in perturbation analysis when we want to investigate properties of the solution, bifurcating from the steady propagating front (see [24] for details).

8. Conclusion. The speed of planar combustion fronts was investigated using the shooting and relaxation methods for different values of Lewis number and different values of β (the ratio of the activation energy to heat release). We have compared the numerical results with the asymptotic estimation of the speed of the combustion front. Derivation of the speed estimation is given in section 3 and agrees with the results of [5, 7, 8]. The correspondence between the numerical and analytical results is good for large β and $\tau \sim 1$, whereas for moderate values of β the difference becomes significant. This is expected, as the asymptotic formula for speed of the front was derived in the leading order of the asymptotic expansion with β being a small parameter. It is also important to note that as we decrease the value of τ up to the order of β^{-1} the asymptotic prediction of the front speed becomes unsatisfactory even for sufficiently large values of β. This reveals the fact that, in the asymptotic treatment of the problem, τ was considered to be of the order of units, and therefore the asymptotic approach fails to work for $\tau \sim \beta^{-1}$. It is interesting to note that the dependence of speed on β seems to be correct, whereas the dependence of c on τ is valid only for $\tau \sim 1$. Excellent correspondence of the numerical results obtained with the integration of the

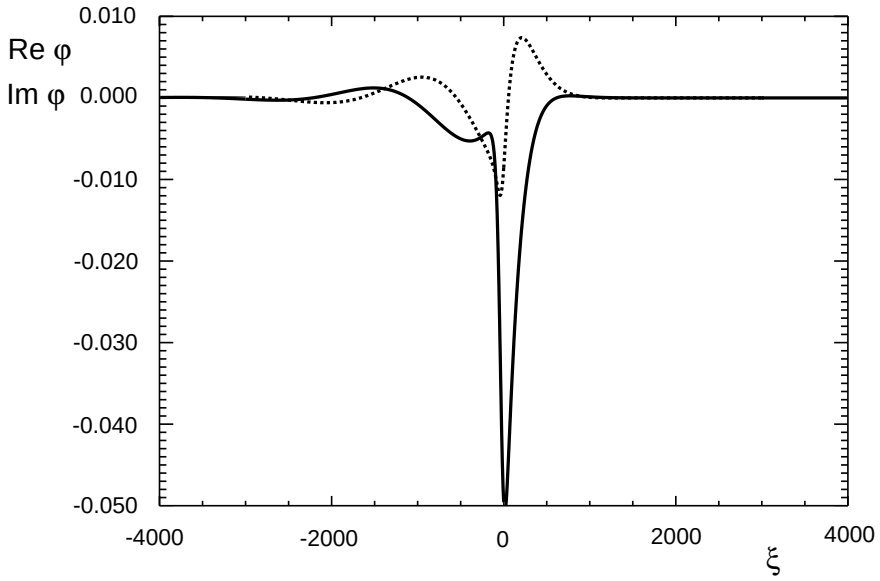

FIG. 7. *The eigenmode $\varphi(\xi)$ of the system* (4.2)–(4.3) *for $\tau = 0.3$, $\beta = \beta_c = 9.7404$, and purely complex eigenvalue $\lambda = i\lambda_c$. The solid line corresponds to Re φ, and the dashed line denotes Im φ.*

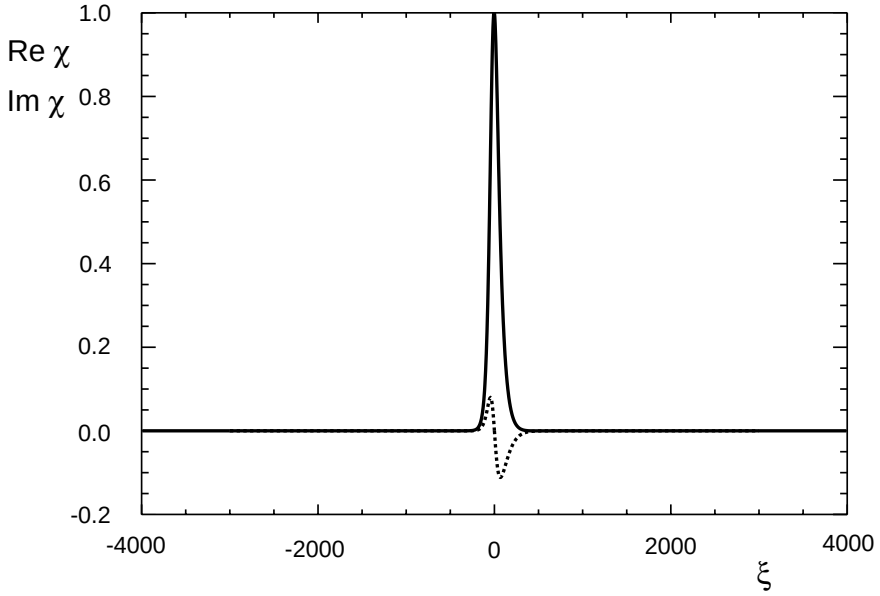

FIG. 8. *The eigenmode $\chi(\xi)$ of the system* (4.2)–(4.3) *for $\tau = 0.3$, $\beta = \beta_c = 9.7404$, and purely complex eigenvalue $\lambda = i\lambda_c$. The solid line corresponds to Re χ, and the dashed line denotes Im χ.*

governing PDE and corresponding ODE supports the credibility of both methods (the difference was found in the third significant digit). At the same time, we believe that the shooting and relaxation methods are preferable, as they require fewer computer resources, are more accurate, and do not depend on the stability of the solution.

The Evans function method was employed to examine the linear stability problem.

In this paper we consider only pulsating instabilities. Methods used in this paper are able to treat cellular instabilities as well (see [14]), and this is the subject of a separate paper. It was shown in section 7 that the conventional method for calculating the Evans function fails in our case. We demonstrated that the compound matrix method significantly expands the applicability of the Evans function approach. The results obtained with the compound matrix method were compared to the predictions of the asymptotic models. It appears that classic asymptotic models derived with truncated series are able to give only qualitative behavior for the front stability. We cannot expect the model derived in [4, 5] to give good quantitative results for $\tau \in [0, 0.6]$ considered in this paper, as it is valid for $\tau \simeq 1$. We would like to mention that it is very difficult to check the results of the asymptotic analysis for $\tau \to 1$ both numerically and experimentally, because the pulsating instability manifests itself only for extremely large values of β in this case. To the best of our knowledge β values of less than 30, considered in this paper while analyzing the stability of the travelling front, cover most of the combustion reactions. It turns out that the results obtained with the generalized matched asymptotic expansion method in [9] best correspond to the numerical data found in the present paper.

The compound matrix method not only allowed us to obtain a simple numerical criterion for the transition to instability for steady propagating solutions, but also provided us with more detailed information about the eigenvalues and eigenmodes. We located the eigenvalues, responsible for transition to instability, on the complex plane and found corresponding eigenmodes for the linear stability problem. This information can be useful, for example, in the analysis of the bifurcating solutions and their stability.

Finally, we would like to say a few words regarding the ambient temperature, which was taken to be equal to zero in this paper. The main disadvantage of this approach is the fact that the ambient temperature is a convenient control parameter used in experiments. This parameter is also ruled out in the asymptotic theories mentioned earlier. Therefore it is of clear interest to investigate the effect of this parameter on the stability of the combustion front. In the future we will be applying the methods described in this paper to models with finite ambient temperature and taking heat loss into consideration.

Acknowledgments. The authors thank S. J. A. Malham and K. Y. Kolossovski for helpful discussions, and the anonymous referees for their useful comments.

REFERENCES

[1] G. I. Sivashinsky, *Structure of Busen flames*, J. Chem. Phys., 62 (1975), pp. 638–643.
[2] G. I. Sivashinsky, *Diffusional-thermal theory of cellular flames*, Combust. Sci. Technol., 15 (1977), pp. 137–146.
[3] B. J. Matkowsky and G. I. Sivashinsky, *Propagation of a pulsating reaction front in solid fuel combustion*, SIAM J. Appl. Math., 35 (1978), pp. 465–478.
[4] B. J. Matkowsky and D. O. Olagunju, *Propagation of a pulsating flame front in a gaseous combustible mixture*, SIAM J. Appl. Math., 39 (1980), pp. 290–300.
[5] S. B. Margolis and B. J. Matkowsky, *Nonlinear stability and bifurcation in the transition from laminar to turbulent flame propagation*, Combust. Sci. Technol., 34 (1983), pp. 45–77.
[6] W. B. Bush and F. E. Fendell, *Asymptotic analysis of laminar flame propagation for general Lewis numbers*, Combust. Sci. Technol., 1 (1970), pp. 421–428.
[7] R. O. Weber, G. N. Mercer, H. S. Sidhu, and B. F. Gray, *Combustion waves for gases ($Le = 1$) and solids ($Le \to \infty$)*, Proc. Roy. Soc. London Ser. A, 453 (1997), pp. 1105–1118.
[8] A. C. McIntosh, R. O. Weber, and G. N. Mercer, *Non-adiabatic combustion waves for general Lewis numbers: Wave speed and extinction conditions*, ANZIAM J., submitted.

[9] D. A. Schult, *Matched asymptotic expansions and the closure problem for combustion waves*, SIAM J. Appl. Math., 60 (1999), pp. 136–155.
[10] J. W. Evans, *Nerve axon equations,* IV: *The stable and unstable impulse*, Indiana Univ. Math. J., 24 (1975), pp. 1169–1190.
[11] T. J. Bridges and G. Derks, *The symplectic Evans matrix, and the instability of solitary waves and fronts with symmetry*, Arch. Ration. Mech. Anal., 156 (2001), pp. 1–87.
[12] A. L. Afendikov and T. J. Bridges, *Instability of the Hocking–Stewartson pulse and its implications for three-dimensional Poiseuille flow*, R. Soc. Lond. Proc. Ser. A Math. Phys. Eng. Sci., 457 (2001), pp. 1–16.
[13] L. A. Allen and T. J. Bridges, *Numerical exterior algebra and the compound matrix method*, Numer. Math., 92 (2002), pp. 197–232.
[14] N. J. Balmforth, R. V. Craster, and S. J. A. Malham, *Unsteady fronts in an autocatalytic system*, R. Soc. Lond. Proc. Ser. A Math. Phys. Eng. Sci., 455 (1999), pp. 1401–1433.
[15] D. Terman, *Stability of planar wave solutions to a combustion model*, SIAM J. Math. Anal., 21 (1990), pp. 1139–1171.
[16] R. L. Pego and M. I. Weinstein, *Evans' function, Melnikov's integral, and solitary wave instabilities*, in Differential Equations with Applications to Mathematical Physics, W. F. Ames, E. M. Harrell II, and J. V. Herod, eds., Academic Press, San Diego, 1993, pp. 273–286.
[17] D. E. Pelinovsky, Y. S. Kivshar, and V.V. Afanasjev, *Internal modes of envelope solitons*, Phys. D, 116 (1998), pp. 121–142.
[18] J. Guckenheimer and P. Holmes, *Nonlinear Oscillations, Dynamical Systems, and Bifurcations of Vector Fields*, Springer-Verlag, New York, 1983.
[19] R. L. Pego, P. Smereka, and M. I. Weinstein, *Oscillatory instability of traveling waves for a KdV-Burgers equation*, Phys. D, 67 (1993), pp. 45–65.
[20] B. S. Ng and W. H. Reid, *An initial value method for eigenvalue problems using compound matrices*, J. Comput. Phys., 30 (1979), pp. 125–136.
[21] B. S. Ng and W. H. Reid, *The compound matrix method for ordinary differential equation*, J. Comput. Phys., 58 (1985), pp. 209–228.
[22] P. G. Drazin and W. H. Reid, *Hydrodynamic Stability*, Cambridge University Press, London, 1981.
[23] V. Gubernov, G. N. Mercer, H. S. Sidhu, and R. O. Weber, *Numerical methods for the analysis of travelling waves in reaction-diffusion equations*, ANZIAM J(E), to appear.
[24] A. I. Volpert, V. A. Volpert, and V. A. Volpert, *Travelling Wave Solutions of Parabolic Systems*, Transl. Math. Monogr. 140, AMS, Providence, RI, 1994.
[25] J. Alexander, R. Gardner, and C. Jones, *A topological invariant arising in the stability analysis of travelling waves*, J. Reine Angew. Math., 410 (1990), pp. 167–212.